Electronic Supplementary Material (ESI) for RSC Advances.

Supporting Information for

Nanocomposite of graphene oxide decorated Al-waste sludge for removal of Rhodamine B from water

Buddini Nissanka [a], Dilushan R. Jayasundara [a,*]

[a] Department of Physics, University of Colombo, Colombo 00300, Sri Lanka.

*Corresponding author: dilushanj@phys.cmb.ac.lk

Characterization of GO and pGO

The structural and chemical characterization of GO and pGO were performed using XRD, Raman, FTIR and XPS spectroscopy, and the resulting spectra are shown in the manuscript as Figure 2. The XRD spectrum of GO in Figure 2 (a) exhibits a sharp peak at $2\theta = 9.76^{o}$, which is typical for GO and corresponds to reported values on similarly prepared samples.[1] The XRD spectrum of GO after subjecting to a thermal treatment at 150 ^{o}C is also shown on the same plot. The absence of the previously observed peak at $2\theta = 9.76°$ for GO and the presence of a low intensity broader peak at $2\theta = 11.7^{o}$ are evidence for partial reduction of GO. Figure 2 (b) shows the Raman spectra of GO and pGO. These spectra consist of intense D (~1350 cm^{-1}) and G (~1585 cm^{-1}) bands with low intense 2D (~2690 cm^{-1}) band. The intense D band is related to the structural defects and disorders within the graphitic layers while G band indicates the in-plane vibration of sp^2 carbon atoms in the two dimensional hexagonal lattice.[2] The 2D band is attributed to the number of graphene layers. Based on the spectral data, the intensity ratio of D and G bands (I_D/I_G) was measured inorder to compare the degree of disorder. The measured I_D/I_G ratio of GO is 0.88 and that of pGO is 0.90. Thus, the increase in the I_D/I_G ratio for pGO indicates the increase of defects during thermal anealing of GO at 150 ^{o}C.

Figure 2 (c) shows the FTIR spectra of GO and pGO. FTIR spectra of GO exhibit a broad band between 3000 – 3700 cm^{-1}, corresponding to the stretching vibrations of O-H from hydroxyl, carboxyl and water adsorbed on GO. The bands appearing at 1806, 1732, 1620, 1235, 1047 and 1380 cm^{-1} correspond to the stretching vibration of C=O, COOH[3,4], C=C[5], C-O-C[6,7] and C-O in C-OH[6], and bending vibrations of C-OH[7,8], respectively. However, the FT-IR spectrum of pGO shows reduction in the intensities of stretching vibrational bands corresponding to O-H and epoxides during the thermal treatment process. This reduction in intensities indicate partial removal of oxygen functionalities during the thermal treatment.

XPS spectra of GO and pGO were obtained to further evaluate the chemical nature of oxygen functionalities as shown in Figure 2 (d). High resolution XPS spectra of C 1s region show two main peaks for both GO and pGO that are similar to the other reported GO samples.[9] The ratios of O bound carbon to total carbon % was calculated using area ratios of these two main peaks. The results indicate a reduction in the O bound carbon to total carbon in pGO (55%) compared to that of GO (61%). These spectral data further confirms the reduction in the oxygen functionalities together with restoration of graphitic structure during partial reduction at 150 ^{o}C.

Average particle size measurement of mAHS

The waste sludge discharged from anodizing industry was dried, ball milled and sieved to obtain mAHS. The mAHS was then analyzed for its average particle size distribution and the results are shown in Figure SI1.

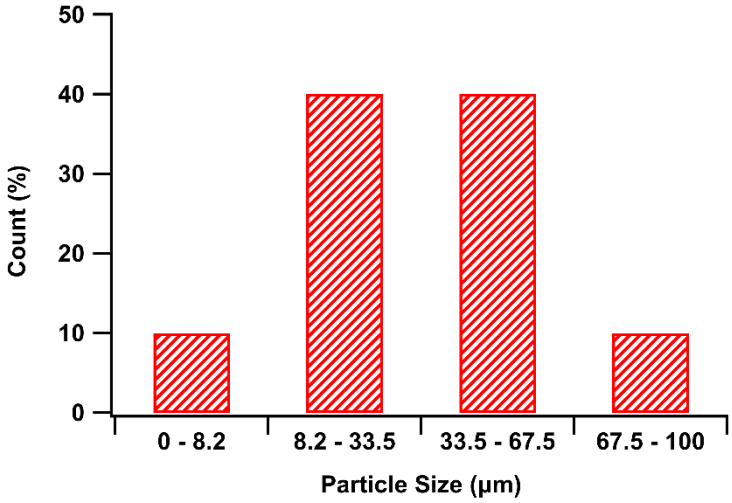

Figure SI1 Particle size distribution of mAHS.

Morphological analysis of the composite

The morphological features of the pGO-mAHS were analyzed using SEM as shown in Figure SI2. This shows the porous structure of mAHS and the flake-like structure of GO, indicating incorporation of GO to composite during the modification process.

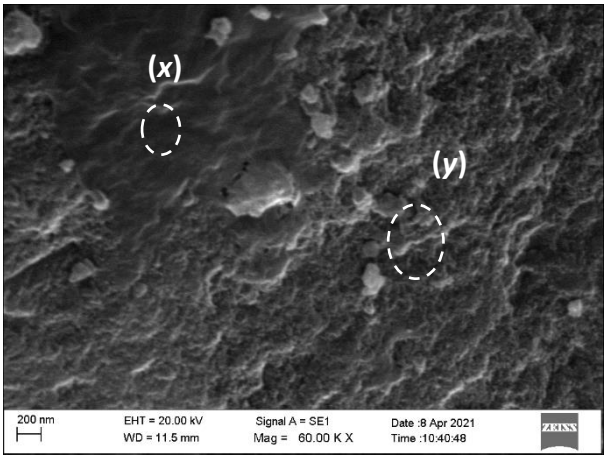

Figure SI2 SEM image of the pGO-mAHS with (*x*) flake-like structure of GO and (*y*) porous structure of sludge.

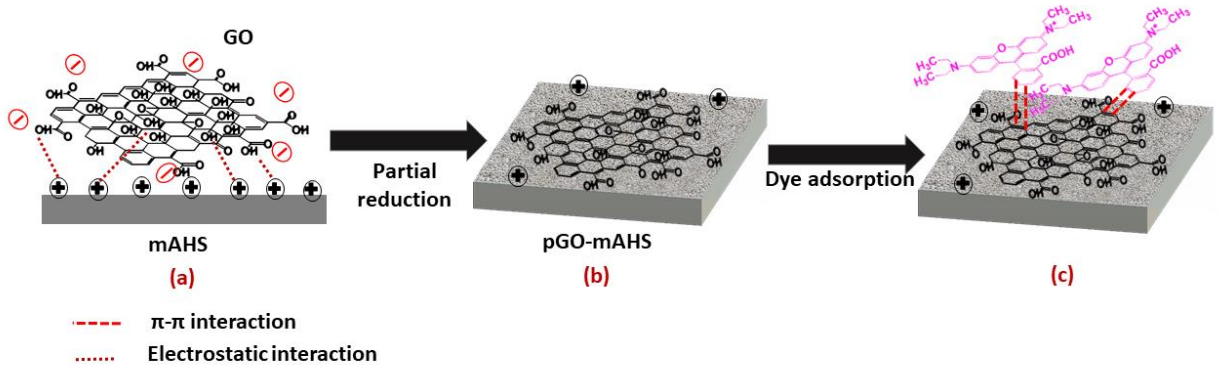

Figure SI3 Schematic representation of the (a) GO-mAHS interactions, (b) pGO-mAHS composite and (c) RhB- composite interactions.

References

1 B. Nissanka, N. Kottegoda and D. R. Jayasundara, *J. Mater. Sci.*, 2019, **55**, 1996–2005.

2 R. Muzyka, S. Drewniak, T. Pustelny, M. Chrubasik and G. Gryglewicz, *Materials (Basel).*, 2018, **11**, 1050.

3 M. Acik, G. Lee, C. Mattevi, A. Pirkle, R. M. Wallace, M. Chhowalla, K. Cho and Y. Chabal, *J. Phys. Chem. C*, 2011, **115**, 19761–19781.

4 G. Venugopal, K. Krishnamoorthy, R. Mohan and S.-J. Kim, *Mater. Chem. Phys.*, 2012, **132**, 29–33.

5 D. C. D. . Marcano, D. . D. V. Kosynkin, J. M. Berlin, A. Sinitskii, Z. Z. Sun, A. Slesarev, L. B. Alemany, W. Lu and J. M. Tour, *ACS Nano*, 2010, **4**, 4806–4814.

6 J. Zhang, H. Yang, G. Shen, P. Cheng, J. Zhang and S. Guo, *Chem. Commun.*, 2010, **46**, 1112–1114.

7 C. Zhang, D. M. Dabbs, L.-M. Liu, I. A. Aksay, R. Car and A. Selloni, *J. Phys. Chem. C*, 2015, **119**, 18167–18176.

8 Y. Si and E. T. Samulski, *Nano Lett.*, 2008, **8**, 1679–1682.

9 D. Perera, A. Abeywickrama, F. Zen, P. E. Colavita and D. R. Jayasundara, *Mater. Chem. Phys.*, 2018, **220**, 417–425.